

## Article

# The Impact of Fast Radiation on the Phylogeny of *Bactrocera* Fruit Flies as Revealed by Multiple Evolutionary Models and Mutation Rate-Calibrated Clock

Federica Valerio <sup>1</sup>, Nicola Zadra <sup>2,3</sup>, Omar Rota-Stabelli <sup>2,3,4</sup> and Lino Ometto <sup>1,\*</sup>

<sup>1</sup> Department of Biology and Biotechnology, University of Pavia, 27100 Pavia, Italy; federica.valerio02@universitadipavia.it

<sup>2</sup> Research and Innovation Centre, Fondazione Edmund Mach, 38010 San Michele all'Adige, Italy; zadranc@gmail.com (N.Z.); omar.rotastabelli@unitn.it (O.R.-S.)

<sup>3</sup> Department of Cellular, Computational and Integrative Biology—CIBIO, University of Trento, 38123 Trento, Italy

<sup>4</sup> Center Agriculture Food Environment—C3A, University of Trento, 38010 San Michele all'Adige, Italy

\* Correspondence: lino.ometto@unipv.it

**Simple Summary:** Comparative approaches are widely used to investigate the traits that underlie particular biological and ecological traits. They are effective, however, only if we know the correct relationships among the species under consideration. Here, we aimed at reconstructing a robust phylogeny for selected true fruit flies of the genus *Bactrocera*, which are well known as important agricultural pests worldwide. Existing phylogenetic inferences are still ambiguous, especially concerning the relationship between the two major pests *B. dorsalis* and *B. tryoni*. In this study, we employed a genome-scaled dataset and different models of molecular evolution to reconstruct the phylogenetic relationships of ten *Bactrocera* species and two outgroups and further date their divergence times. The resulting phylogeny fully supports *B. dorsalis* as more closely related to *B. latifrons* than to *B. tryoni*, opposite to what was supported by previous works. This incongruence likely derives from a fast divergence of these lineages, as revealed by our clock analysis, which can lead to conflicting results when using few genetic markers. Our results thus highlight the utility of using large datasets and of exploring different evolutionary models to study the evolutionary history of species of economic importance.

**Abstract:** Several true fruit flies (Tephritidae) cause major damage to agriculture worldwide. Among them, species of the genus *Bactrocera* are extensively studied to understand the traits associated with their invasiveness and ecology. Comparative approaches based on a reliable phylogenetic framework are particularly effective, but several nodes of the *Bactrocera* phylogeny are still controversial, especially concerning the reciprocal affinities of the two major pests *B. dorsalis* and *B. tryoni*. Here, we analyzed a newly assembled genomic-scaled dataset using different models of evolution to infer a phylogenomic backbone of ten representative *Bactrocera* species and two outgroups. We further provide the first genome-scaled inference of their divergence by calibrating the clock using fossil records and the spontaneous mutation rate. The results reveal a closer relationship of *B. dorsalis* with *B. latifrons* than to *B. tryoni*, contrary to what was previously supported by mitochondrial-based phylogenies. By employing coalescent-aware and heterogeneous evolutionary models, we show that this incongruence likely derives from a hitherto undetected systematic error, exacerbated by incomplete lineage sorting and possibly hybridization. This agrees with our clock analysis, which supports a rapid and recent radiation of the clade to which *B. dorsalis*, *B. latifrons* and *B. tryoni* belong. These results provide a new picture of *Bactrocera* phylogeny that can serve as the basis for future comparative analyses.

**Keywords:** *Bactrocera*; phylogenomics; phylogeny; dating; incomplete lineage sorting; *Bactrocera dorsalis*; *Bactrocera tryoni*



**Citation:** Valerio, F.; Zadra, N.; Rota-Stabelli, O.; Ometto, L. The Impact of Fast Radiation on the Phylogeny of *Bactrocera* Fruit Flies as Revealed by Multiple Evolutionary Models and Mutation Rate-Calibrated Clock. *Insects* **2022**, *13*, 603. <https://doi.org/10.3390/insects13070603>

Academic Editors: David S. Haymer and Teresa Vera

Received: 29 April 2022

Accepted: 28 June 2022

Published: 30 June 2022

**Publisher's Note:** MDPI stays neutral with regard to jurisdictional claims in published maps and institutional affiliations.



**Copyright:** © 2022 by the authors. Licensee MDPI, Basel, Switzerland. This article is an open access article distributed under the terms and conditions of the Creative Commons Attribution (CC BY) license (<https://creativecommons.org/licenses/by/4.0/>).

## 1. Introduction

Tephritidae, commonly known as true fruit flies, are an incredibly diverse group of phytophagous insects. This family includes more than 5000 species in over 500 genera [1], making it one of the largest among Diptera. Several of these species cause extensive damage to agriculture worldwide, since females lay eggs within the fruit flesh (i.e., pericarp) and the larvae rapidly develop in the fruit, eating it and inducing bacterial and fungal decay. The accompanying economic impacts are considerable: for instance, the olive fruit fly, *Bactrocera oleae* (Rossi), has been estimated to cause an annual economic loss of approximately \$800 million in the Mediterranean basin alone [2]. Moreover, such impact is exacerbated by these species' ability to invade new areas and establish viable populations. For example, *Bactrocera dorsalis* and *Bactrocera latifrons*, both native to South-East Asia, have recently expanded their distribution range in the Hawaiian Islands [3,4], in several sub-Saharan African countries [5–12], and also in Europe [9,13,14], where they are posing an immediate or potential threat to local agriculture.

Most relevant tephritid pests belong to five genera: *Anastrepha* Schiner, *Ceratitidis* MacLeay, *Rhagoletis* Loew, *Zeugodacus* Hendel and *Bactrocera* Macquart. The genus *Bactrocera* is the most economically important and comprises over 450 species [15], at least 50 of which are considered important pests [16,17]. Identifying the key ecological and biological traits relevant for their invasiveness and host preference is extremely important to drive effective control strategies. To this aim, comparative approaches based on a reliable phylogenetic framework are particularly effective, as they allow to trace the evolution of species-specific and shared traits and evaluate whether and to what extent control measures may be applied in related species [18]. The *Bactrocera* genus is subdivided into subgenera, species groups and species complexes, and the relationships between these groups have been repeatedly revised (see, e.g., [19–25]). Different molecular phylogenies of *Bactrocera* resulted in different relationships depending on the type (nuclear and/or mitochondrial) and number of markers, and on the number of taxa analyzed [23–29]. For instance, based on mtDNA data, *B. dorsalis* is usually considered to be more closely related to *B. tryoni* than to *B. latifrons* (e.g., [30,31]), but recent studies suggested a poorly supported closer relationship between *B. dorsalis* and *B. latifrons* [24,26,32] (Figure 1a). This uncertainty may also be important for studies relevant for their management, since different phylogenetic reconstructions may affect the interpretation of comparative morphological and genomic studies that focus on pest-related biological traits.

Here, we employed a rigorous phylogenomic approach to infer the phylogeny of ten representative *Bactrocera* species, including seven of the nine major agricultural pests of worldwide importance (see Table 1 in [16]), and we calibrated a relaxed clock to estimate their divergences. Rather than resolving the full *Bactrocera* phylogeny, our aim is to provide a robust phylogenetic and chronological backbone that can clarify the yet unresolved (*B. dorsalis*, *B. tryoni*, *B. latifrons*) clade, and which can then serve as basis for powerful comparative analyses. Our dataset also includes species characterized by distinct diets, which range from polyphagy (e.g., *B. dorsalis*) to monophagy (e.g., *B. oleae*), and, therefore, understanding the evolutionary history of this group may also provide precious information on the mode and tempo of the evolution of their biology and ecology.

## 2. Materials and Methods

### 2.1. Datasets

In our analysis, we included *Bactrocera* and Dacini species for which genomic and/or transcriptomic resources were available: *Bactrocera jarvisi* (Tryon), *Bactrocera oleae* (Rossi), *Bactrocera minax* (Enderlein), *Bactrocera bryoniae* (Tryon), *Bactrocera correcta* (Bezzi), *Bactrocera dorsalis* (Hendel), *Bactrocera latifrons* (Hendel), *Bactrocera musae* (Tryon), *Bactrocera tryoni* (Froggatt), *Bactrocera zonata* (Saunders) and *Zeugodacus cucurbitae* (Coquillett). In particular, we analyzed datasets of coding sequences (CDS) and of RNA (transcript) sequences for *Ceratitidis capitata* [33], *Z. cucurbitae* [34], *B. dorsalis* [35], *B. latifrons* (NCBI accession: MIMC00000000.1), *B. minax* [36] and *B. oleae* [37]. For the six remaining *Bactrocera* species

(*B. bryoniae*, *B. correcta*, *B. jarvisi*, *B. musae*, *B. tryoni* and *B. zonata*), we downloaded the available RNA-Seq raw reads (see Table S1 for SRA accession numbers) and assembled the corresponding transcriptomes using default parameters with Trinity v. 2.7.0 [38].

## 2.2. Orthologous Gene Set Identification and Alignment

Orthologs across the ten *Bactrocera* species and the outgroups *Z. cucurbitae* and *C. capitata* were identified using a reciprocal-best-hit approach using pairwise BLASTn searches [39] between the *C. capitata* CDS sequences and each of the other datasets. Putative 1:1 orthologs were first aligned using MAFFT [40] and any incomplete codon (based on the *C. capitata* sequence) was removed. We then re-aligned the ortholog sets using the PRANK algorithm [41] implemented in the tool TranslatorX [42]. We minimized bias in our datasets by 1) removing alignments containing sequences with internal stop codons and 2) using a custom perl script to remove problematic and ambiguous alignment regions [43]. Using this pipeline, we ultimately identified 110 orthologous gene sets across all twelve species (single alignments are available as Supplementary File S1).

We concatenated orthologs to generate an alignment of 189,891 nucleotides (nts) and then translated it using the standard genetic code to obtain an alignment of 63,297 amino acids (aas). We further generated an alignment of 24,885 nts containing only 4-fold degenerate sites retrieved using MEGA7 [44].

## 2.3. Phylogenetic Analyses

We inferred phylogenetic relationships using both a maximum likelihood (ML) and a Bayesian approach. To explore possible sources of systematic errors, we employed homogenous, heterogeneous and coalescent-aware models of evolution.

We ran ML analyses on both the concatenated aa alignment using the PROTGAM-MAGTR model, and on the nt alignment partitioned in first, second and third (1 + 2 + 3) position using the GAMMAGTR model implemented in RAxML [45]. We also ran an ML analysis based on the 4-fold degenerate site alignment using the GAMMAGTR model. In all cases, node support was calculated by the rapid bootstrap feature of RAxML (100 replicates). We also estimated bootstrap supports using the coalescent-aware analysis of ASTRAL [46], which was based on all single ML gene trees obtained by RAxML using the same models of the concatenated analyses for either the nt or the aa sequences. Bootstrap values were estimated by performing either 100 multi-locus bootstrap replicates or gene + site resampling (using the -g option).

The same three datasets, aas, nts (1 + 2 + 3), and 4-fold degenerate sites, were used to run Bayesian analyses in BEAST v. 2.5.1 [47]. The aminoacidic dataset was analyzed with a LG + G4 substitution model. The 4-fold degenerate site dataset and the codon dataset were analyzed with a GTR + G4 substitution model. The codon dataset was split into three partitions, corresponding to the codon positions, setting linked trees across them. We performed additional Bayesian analysis on the aminoacidic dataset using a CAT + GTR model and on the 4-fold degenerate site dataset using the among-site heterogeneous CAT model with gamma distribution with PhyloBayes [48]. In both cases, we ran two independent MCMC chains and checked for convergence using the associated tracecomp and bpcomp commands. For the aminoacidic dataset we let both chains run until parameters were stabilized with  $maxdiff = 0$ ,  $reldiff < 0.2$  (except for *loglik*, *alpha*, *stat* and *rrent*, with  $reldiff$  between 0.62 and 0.77) and the effective sample size was  $effsize > 170$  (except for *loglik*, *alpha*, *stat*, *rrent* and *allocent*, with  $effsize$  between 16 and 119). For the 4-fold degenerate site dataset, both chains ran until parameters were stabilized with  $maxdiff = 0$ ,  $reldiff < 0.25$  (except for *stat*, with  $reldiff < 0.4$ ) and the effective sample size was  $effsize > 170$  (except for *nmode*, *statalpha*, *kappa* and *allocent*, with  $effsize$  between 17 and 85). The summary statistics reached stability at the end of the runs and were periodically visualized with the script graphphylo (<https://github.com/wrf/graphphylo> accessed on 15 April 2022).

Bayesian analyses were also ran using StarBEAST2 [49], which employs a multispecies coalescent method to estimate species trees from multiple sequence alignments, as im-

plemented in the BEAST2 package and according to the tutorial provided by Taming the BEAST2 [50]. For this analysis we used either the nucleotide or the aminoacidic alignments, linking the site models across the gene sets.

BEAST2 and StarBEAST2 analyses had chains run for  $10^8$  generations (or until convergence for at least  $4 \times 10^7$  generations), sampling trees and parameters every 1000 generations and inspecting convergence and likelihood plateauing in Tracer. Posterior consensus trees were generated after discarding the first 10% of generations as burn-in. For the StarBEAST2 analysis, single-gene trees were loaded and visualized by DensiTree [51].

#### 2.4. Dating Analysis

Because of the numerous incongruences between the species tree obtained by the multi-locus analyses and the single-gene trees (see Section 3), which could bias the dating analysis, we produced a conservative dataset by: (i) limiting the species sample to 10 representative species (*C. capitata*, *Z. cucurbitae*, *B. bryoniae*, *B. dorsalis*, *B. jarvisi*, *B. latifrons*, *B. minax*, *B. musae*, *B. oleae*, *B. tryoni*) and (ii) considering only those 37 genes that produced a ML tree supporting the consensus species tree with minimum ML bootstrap values of 50 at each node.

Divergence times were then estimated by BEAST v. 2.5.1 using the 4-fold degenerate sites of the resulting concatenated dataset (11,768 nt). We calibrated the crown of the Dacinae (*Ceratitis-Bactrocera* split) by setting a root prior uniformly distributed between 6 and 65 million years ago, which correspond to the age of a *Ceratitis* fly fossil [52] and of the Schizophora radiation [53,54], respectively. The exact placement of fossils is often disputed and, in general, fossils are also misused because phylogenetic models generally use them to calibrate nodes even though they represent extinct lineages on the stem and not the exact ancestors of the extant ones. In light of this, the mutation rate represents an alternative valid calibration. Indeed, the 4-fold degenerate site dataset also allowed us to use a spontaneous (neutral) mutation rate as an additional prior. Since mutation rate in Tephritidae is not known yet, we assumed it to be similar to that of *Drosophila* (another Diptera) and used the estimate of 0.0346 (SD = 0.0028) substitutions per base pair per million years, provided in [55,56]. This assumption is reasonable, as the mutation rate of insects is quite conserved, with the spontaneous mutation rate of *Heliconius melpomene* (Lepidoptera) being very close to that of *D. melanogaster* ( $2.9 \times 10^{-9}$  and  $3 \times 10^{-9}$ , respectively [57,58]). In addition, the large SD derives from the error associated with the mutation rate estimate and, thus, also accounts for the between-branch variation in substitution rates. Because in *Bactrocera* we assumed eight generations per year (in nature they range from 3 to 5 of *B. oleae* and sub-tropical *B. dorsalis* populations, to >12 for the tropical species; [59–62]) and to account for uncertainty, we finally set as prior a normally distributed mean of 0.028 (SD = 0.03). In a second approach, we set a mutation rate log-normally distributed with “mean in real space”  $M = 0.028$  and  $S = 0.82$  (to produce the same 95% quantile, 0.077, as the normal distribution). For both approaches we performed a model selection to choose the most fitting clock and demographic prior based on the marginal likelihood values with the nested sampling approach implemented in the NS package [63]. We tested the strict and the LOGN relaxed clock and the Yule and the birth–death models, for a total of eight different combinations. Following the recommendations provided by the dedicated Taming the Beast tutorial [50], the sub-chain length was set at 50,000, which corresponds to the length of the MCMC run (i.e.,  $5 \times 10^7$ ) divided by the smallest ESS value observed across the eight model runs (i.e., ~1000), and the number of particles was set at 10. A model was considered favored over another if the difference between the two marginal likelihoods (i.e., the Bayes factor (BF) in log space) was more than twice the sum of the corresponding standard deviations. We ran eight different analyses that used different combinations of priors and model settings and performed a model selection to identify the most appropriate for our data. In particular, the nested sampling approach allowed us to estimate the marginal likelihoods of the different models and make pairwise comparisons using the associated Bayes factor. All models had marginal likelihoods with a standard

deviation ranging from 2.5 to 2.9, which was small enough to assess whether a model was favored over another one. In all cases, we employed a GTR + G replacement model. Because the Bayesian phylogenetic analysis on the concatenated 4-fold degenerate sites resulted in a topology incongruent to the one supported by all other ML and Bayesian analyses (see Section 3), the species tree was fixed according to the consensus topology.

All analyses were performed twice, with chains ran for  $5 \times 10^7$  generations, sampling trees and parameters every 1000 generations and inspecting convergence and likelihood plateauing in Tracer. Both chains resulted well mixed, with average effective sample size (ESS) values across posterior values being well above 200. The consensus trees (maximum clade credibility trees) were generated after discarding the first 20% of generations as burn-in.

### 3. Results

#### 3.1. Phylogenetic Analysis

The results of our analyses strongly indicate that *B. dorsalis* is more closely related to *B. latifrons* than to *B. tryoni* (Figure 1). This relationship is highly supported according to both the ML bootstrap values ( $\geq 98$ , Figures 1a and S1) and the Bayesian posterior probabilities obtained using both BEAST and PhyloBayes analyses (PP = 1, Figures 1a and S2–S4), no matter whether they were based on the codon or aminoacidic alignments. The only support for the relationship (*B. dorsalis*, *B. tryoni*), *B. latifrons*) comes from the Bayesian analysis run in BEAST2 and was based on the concatenated alignment of the 4-fold degenerate sites (Figure S5). This latter dataset contains sites under (nearly) neutral evolution and, therefore, is suitable for divergence time estimates because it allows a calibration in which a neutral spontaneous mutation rate can be considered equal to the substitution rate [18,56]. This type of dataset is, however, more prone to saturation, and hence, artefacts due to systematic errors. When the 4-fold degenerate site dataset was analyzed in PhyloBayes (which is also a Bayesian implementation) using the among-site heterogeneous CAT model, instead of the among-site GTR homogenous model in BEAST2, we retrieved the same topology obtained by the aforementioned Bayesian and ML analyses on the nucleotide and aminoacidic datasets (Figure S6; see also Figure S7 for the results of the ML analysis on the same dataset). Heterogeneous models such as CAT can accommodate for systematic errors related to site-specific variation of the replacement pattern: this suggests that the discordant topology obtained by BEAST2, and also supported by mitochondrial data, is likely an artefact due to model inadequacy.

#### 3.2. Dating Analysis

Our dating analysis is based on the best combination of priors according to a model selection whose results (Table S2) indicated as the favored model the one where we set the mutation prior with a log-normal distribution, a strict clock, and a birth–death model. The Bayes factor values, even after correcting for uncertainty by subtracting the corresponding standard deviations, were well above two, which provides overwhelming support for that model [64]. The fact that a strict clock is favored over a relaxed clock is consistent with the low mean value of the coefficient of variation parameter (i.e., the standard deviation of branch rates divided by the mean rate), which equals 0.24. Therefore, in the main text we report and discuss the results obtained by this analysis.

The clade including *Zeugodacus* and *Bactrocera* split from *Ceratitidis* between 6 and 45 million years ago (mean 19 million years ago, mya; 95% highest posterior density, 95%HPD, of 6–45 mya; Figure 2), with *Zeugodacus* then diverging ca. 7.6 mya (95%HPD: 2.3–18 mya). The diversification of *Bactrocera* followed immediately after, ca. 5.9 mya (95%HPD: 1.8–14 mya), with a rapid radiation subtending the species-rich clade [24] that includes the polyphagous species *B. dorsalis*, *B. latifrons* and *B. tryoni* happening between ca. 2.1–1.9 mya (95%HPDs 0.6–5 mya).

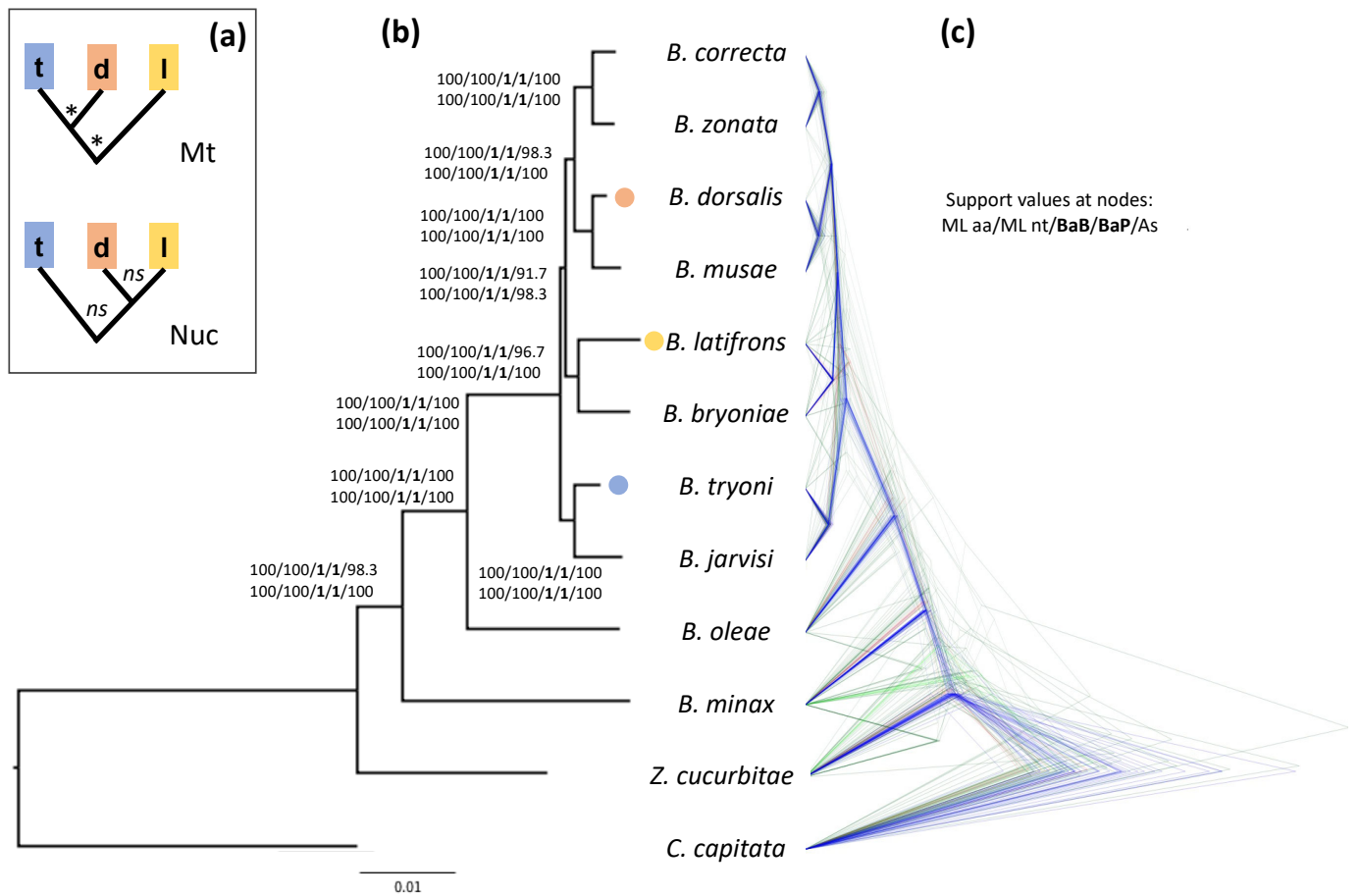


**Figure 1.** Phylogeny of *Bactrocera* inferred from the aminoacidic alignments of 110 orthologous nuclear genes. (a) Alternative phylogenetic relationships with supported (\*) and non-supported (ns) nodes between *B. dorsalis* (d), *B. latifrons* (l) and *B. tryoni* (t) as presented in the literature and based on mitochondrial (Mt) DNA (e.g., [30,31]) or nuclear (Nuc) DNA (e.g., [24,26,32]). (b) Phylogeny obtained using a maximum likelihood phylogenetic analysis on the concatenated aminoacidic alignments (63,297 aa). Support at nodes is given as bootstrap values for the ML analyses (both for the aminoacidic and nucleotide alignments), bootstrap values estimated by performing 100 multi-locus gene + site resampling using a multi-locus coalescent-aware phylogenetic analysis in ASTRAL across all 110 genes (As) and as posterior probabilities for the Bayesian BEAST2 and PhyloBayes analyses on the aminoacidic dataset (BaB and BaP, respectively). *Bactrocera dorsalis*, *B. latifrons* and *B. tryoni* tips are color-coded as in panel A. (c) Bayesian analysis obtained by StarBEAST2, which employs a multispecies coalescent method to estimate species trees from multiple sequence alignments (i.e., one for each of the 110 orthologous gene sets). For this analysis we used the aminoacidic alignments, linking the site models across the gene sets. Note the numerous discordant gene trees, especially within the *B. dorsalis*–*B. latifrons*–*B. tryoni* clade, compared to the species tree (supported by the gene trees in blue).

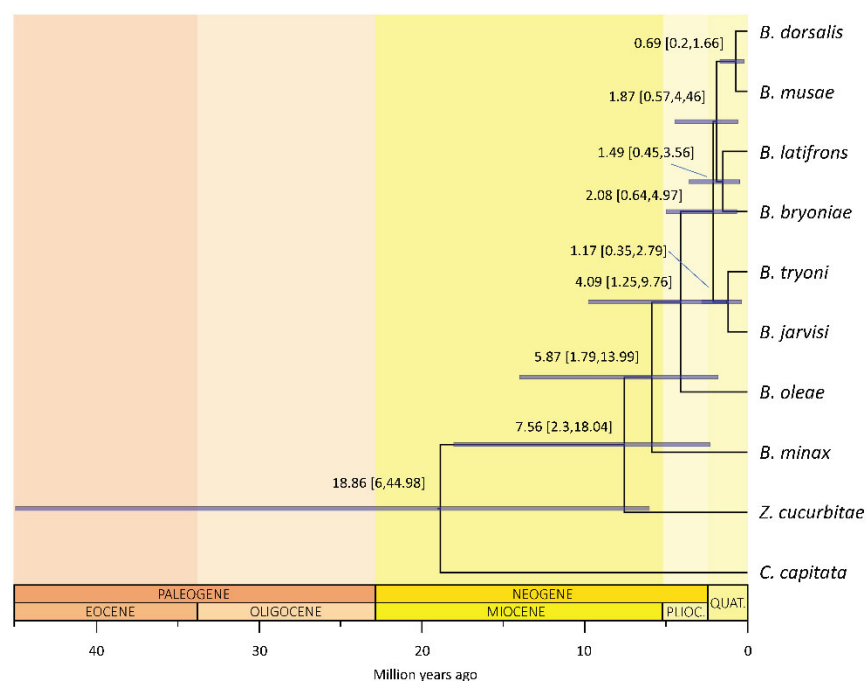


**Figure 2.** Molecular time tree of *Bactrocera*. *Bactrocera* (plus *Zeugodacus*) likely originated during the Miocene optimum (around 19 mya) and experienced recent, fast cladogenetic events less than 5 mya. The analysis was conducted setting the mutation rate log-normally distributed as prior, a strict clock and a birth–death model. Mean and 95% highest posterior density of the inferred age (blue bars) are reported for each node.

#### 4. Discussion

##### 4.1. Phylogenetic Analyses Reveal a Closer Affinity of *B. dorsalis* to *B. latifrons* Than to *B. tryoni*

The results of the phylogenetic analyses reveal relationships that are in contrast with all phylogenies inferred from mitochondrial sequences (e.g., [30,31]), which support *B. dorsalis* as being more closely related to *B. tryoni* than to *B. latifrons*. The results are instead consistent with a closer relationship between *B. dorsalis* and *B. latifrons*, as only partially supported by three previous studies. The first of such phylogenetic analyses, based on 167 Dacini species including *Bactrocera* [24], however, was not conclusive in determining the relationships between these three species, since the phylogeny had many unresolved nodes, including those relative to the most common ancestors of *B. dorsalis*, *B. latifrons* and *B. tryoni*. The low power to disentangle such relationships likely derives from the small dataset—seven nuclear genes—used to produce their phylogeny. A second study by Choo and colleagues [32] analyzed 116 orthologous genes across 11 *Bactrocera* species: despite the larger dataset, their results were also not adequately supported, as the split between (*B. dorsalis*, *B. latifrons*) and *B. tryoni* in a ML analysis had a bootstrap value of 70, indicating lack of statistical confidence. We also note that the incongruence does not extend to the species that in our analyses are identified as the closest relatives to *B. dorsalis* (i.e., *B. musae*), *B. latifrons* (i.e., *B. bryoniae*) and *B. tryoni* (i.e., *B. jarvisi*), and which are characterized by a longer divergence history (see below). Similarly, a third study [26] that produced an even larger phylogenomic dataset using highly multiplexed amplicon sequencing was not conclusive regarding the relationships between these three species, with a polymorphism-aware phylogenetic model [65] analysis favoring *B. dorsalis* being more closely related to *B. tryoni* than to *B. latifrons*, and an ASTRAL analysis in which this relationship was unresolved.

The discordance between the results obtained by previous studies and our study points to a complex evolutionary history of the group, as suggested by coalescent-aware analyses. Combining single-gene analyses into a coalescent framework also supports *B. dorsalis* as being more closely related to *B. latifrons* than to *B. tryoni*, both when using

ASTRAL and StarBEAST2 (Figures S8–S13). It is evident, however, that many genes have phylogenies not consistent with the inferred species phylogeny. For instance, the StarBEAST2 approach reveals a high number of genes having an alternative phylogeny within the ((*B. dorsalis*, *B. latifrons*), *B. tryoni*), suggesting incomplete lineage sorting due to fast radiation or (ongoing) hybridization. For example, in the nucleotide datasets, 58 genes have a ((*B. dorsalis*, *B. latifrons*), *B. tryoni*) topology, 38 a ((*B. dorsalis*, *B. tryoni*), *B. latifrons*) topology and 14 a ((*B. tryoni*, *B. latifrons*), *B. dorsalis*) topology. This uncertainty is also apparent in the ASTRAL results, whereby the support for such a clade falls to <92 when bootstrapping by gene resampling (compare Figures S8 and S9). In the light of these results, we cannot exclude the possibility that these species experienced and still experience hybridization events, which could then result in widespread introgression events. Indeed, hybrids have been reported for several closely related *Bactrocera* species [66–76], and although none of the published studies involved the pair of species analyzed in our analyses, possible introgression can occur via direct hybridization or via intermediate hybridization events involving other closely related species. Finally, our results are also consistent with biogeography data: *B. dorsalis* and *B. latifrons* are originally from South Asia, whereas *B. tryoni* is native of Australia, suggesting that their ancestral distributional range also reflects their degree of evolutionary divergence.

#### 4.2. Dating Analysis Suggests Fast and Recent Radiation in *Bactrocera*

Incomplete lineage sorting is expected for rapid radiations (e.g., [77]): this is exactly what is revealed by our molecular clock analyses, which support more recent divergences for the *Bactrocera* radiation compared with previous estimates [23,32,78,79]. Consistent with a rapid radiation of the (*B. dorsalis*, *B. latifrons*, *B. tryoni*) clade, the results of the clock analysis place its origin in the mid-Pliocene, with a mean at ~2.08 mya (95%HPD: 0.6–5 mya), and a subsequent, very close cladogenesis centered at ~1.87 mya (95%HPD: 0.6–4.5 mya) separating *B. dorsalis* and *B. latifrons* (Figure 2; see also Figures S14–S21 for the time trees obtained using the different models reported in Table S2). Interestingly, during this period the sea rose at peak levels [80] and, thus, increased distances between islands and island groups, possibly facilitating allopatric speciation (the three species have native ranges in southeastern Asia and Australia). The proximity of the two cladogenetic events and the large overlap of their 95% confidence intervals agree with a rapid radiation, which could have resulted not only in frequent incomplete lineage sorting but also in possible hybridization events as discussed above. This would also explain the discordant results between the nuclear and the mitochondrial phylogenies, a finding that is reported in many organisms, including insects [81–84].

Our results also revealed that the split between *Zeugodacus* + *Bactrocera* and *C. capitata* could have occurred between 6 and 45 million years ago (mean of ca. 19 mya). Previously published works proposed more ancient *C. capitata* and *Bactrocera* splits at around 24.9 mya (no confidence intervals reported, [78]), 83 mya (95% highest posterior density: 64–103 mya [79]), and 110.9 mya (95% confidence interval: 91.2–131.4 mya [23]). The difference in the estimates could be due to several factors such as the type of molecular markers (nuclear or mitochondrial), the choice of clock and demographic models, and more importantly, the type of calibrations employed. Here we employed a strategy based on a calibration that combined fossil data and mutation rate, in which we assumed a defined number of generations per year on the basis of available demographic evidence [59–62]. Generation time can, however, greatly influence the divergence time estimation: for example, if in our analysis we had assumed five generations per year (instead of eight) without changing the other parameters, the mean divergence time would increase from ~20 to ~32 mya for the *Bactrocera*–*Ceratitidis* split. The latter is close to what was estimated by Choo and colleagues [32], who performed phylogenetic and dating analyses concatenating nuclear ( $n = 116$ ) and mitochondrial ( $n = 13$ ) genes of a similar species dataset and whose divergence time confidence intervals for this node partially overlap with ours (31.21 mya, 95%HPD: 41.27–21.61; this study: 18.86 mya, 95%HPD: 6–44.98). We also employed a

mutation rate prior [55] for the 4-fold degenerate sites that is different and, in our opinion, more conservative than the calibration used by Choo and colleagues. The molecular clock is known to change among sites and lineages [85] and through time [86,87]. Therefore, when choosing a rate prior it is important that it refers to a similar timescale, and especially to sites that evolve similarly. Our approach used a molecular rate estimated from *Drosophila*, which has a generation time and a phylogeny timescale similar to *Bactrocera*; hence, the 4-fold degenerate site rate prior may indeed be a reliable assumption. In contrast, Choo and colleagues used a different approach, whereby they specified as prior only the divergence between *Rhagoletis* (Diptera: Tephritidae) and *Drosophila*, previously inferred in [88].

Finally, we would also like to point out that the mutation rate prior distribution can be a strong determinant of the divergence time estimates and, therefore, need to be carefully tested against alternative models (Table S2): for example, mean divergence time between *C. capitata* and *Bactrocera* is estimated between 18.3 and 18.9 mya when using a log-normal distribution (Figures 2 and S13–S16), whereas it is estimated between 13 and 13.2 mya using a normal distribution (Figures S17–S21), and the same reduction of ~30% holds for all other divergence times across the phylogeny. Nevertheless, model selection indicates that a log-normal is the most fitting prior distribution of the rate; therefore, the divergence times depicted in Figure 2 should be regarded as more likely. Irrespective of the divergence estimate for the deep splits, our results clearly indicate that the clade to which *B. dorsalis*, *B. latifrons* and *B. tryoni* belong underwent a rapid and recent diversification.

## 5. Conclusions

Overall, our clock analyses reveal a recent and fast radiation scenario of *Bactrocera* evolution and our phylogeny provides a useful framework for future comparative genomics and comparative biology studies in the major *Bactrocera* pest species. The possibility that hybridization can still occur between closely related species also warns about the possibility that selective events in one species (for instance, resistance to insecticides) may be readily transferred to other species by introgression. More generally, our results once again highlight the importance of comparing different evolutionary models to understand complex phylogenies.

**Supplementary Materials:** The following supporting information can be downloaded at: <https://www.mdpi.com/article/10.3390/insects13070603/s1>, Figure S1: Phylogeny of *Bactrocera* obtained by RAxML on the concatenated codon alignments; Figure S2: Phylogeny of *Bactrocera* obtained by BEAST2 using a Bayesian analysis on the concatenated aminoacidic alignments; Figure S3: Phylogeny of *Bactrocera* obtained by BEAST2 using a Bayesian analysis on the concatenated codon alignments; Figure S4: Phylogeny of *Bactrocera* obtained by PhyloBayes using a Bayesian analysis on the concatenated aminoacidic alignments; Figure S5: Phylogeny of *Bactrocera* obtained by BEAST2 using a Bayesian analysis on the 4-fold degenerate sites of the concatenated alignments; Figure S6: Phylogeny of *Bactrocera* obtained by PhyloBayes using a Bayesian analysis on the 4-fold degenerate sites of the concatenated alignments; Figure S7: Phylogeny of *Bactrocera* obtained by RAxML using a maximum likelihood analysis on the 4-fold degenerate sites of the concatenated alignments; Figure S8: Phylogeny of *Bactrocera* inferred using ASTRAL and based on single-gene aminoacidic alignments obtained by RAxML and with bootstrap values estimated by performing multi-locus bootstrap replicates; Figure S9: Phylogeny of *Bactrocera* inferred using ASTRAL and based on single-gene aminoacidic alignments obtained by RAxML and with bootstrap values estimated by performing gene + site resampling; Figure S10: Phylogeny of *Bactrocera* inferred using ASTRAL and based on single-gene codon alignments obtained by RAxML and with bootstrap values estimated by performing multi-locus bootstrap replicates; Figure S11: Phylogeny of *Bactrocera* inferred using ASTRAL and based on single-gene codon alignments obtained by RAxML and with bootstrap values estimated by performing gene + site resampling; Figure S12: Multi-locus phylogenesis of *Bactrocera*. Bayesian analyses obtained by StarBEAST2 for each of the aminoacidic orthologous genes alignments; Figure S13: Multi-locus phylogenesis of *Bactrocera*. Bayesian analyses were obtained by StarBEAST2 for each of the codon orthologous genes alignments; Figure S14: Molecular time tree of *Bactrocera* obtained by BEAST2 using the 4-fold degenerate sites using a mutation rate log-normally distributed

as prior, a log-normal clock and a birth–death model; Figure S15: Molecular time tree of *Bactrocera* obtained by BEAST2 using the 4-fold degenerate sites using a mutation rate log-normally distributed as prior, a strict clock and a birth–death model; Figure S16: Molecular time tree of *Bactrocera* obtained by BEAST2 using the 4-fold degenerate sites using a mutation rate log-normally distributed as prior, a log-normal clock and a Yule model; Figure S17: Molecular time tree of *Bactrocera* obtained by BEAST2 using the 4-fold degenerate sites using a mutation rate log-normally distributed as prior, a strict clock and a Yule model; Figure S18: Molecular time tree of *Bactrocera* obtained by BEAST2 using the 4-fold degenerate sites using a mutation rate normally distributed as prior, a log-normal clock and a birth–death model; Figure S19: Molecular time tree of *Bactrocera* obtained by BEAST2 using the 4-fold degenerate sites using a mutation rate normally distributed as prior, a strict clock and a birth–death model; Figure S20: Molecular time tree of *Bactrocera* obtained by BEAST2 using the 4-fold degenerate sites using a mutation rate normally distributed as prior, a log-normal clock and a Yule model; Figure S21: Molecular time tree of *Bactrocera* obtained by BEAST2 using the 4-fold degenerate sites using a mutation rate normally distributed as prior, a strict clock and a Yule model; Table S1: SRA databases used to reconstruct the transcriptome of five *Bactrocera* species; Table S2: Results of the model selection of the different BEAST analyses used to estimate divergence times; File S1: alignments of the 110 orthologous gene sets.

**Author Contributions:** Conceptualization, L.O.; methodology, F.V., N.Z., O.R.-S. and L.O.; formal analysis, F.V., N.Z. and L.O.; investigation, F.V., N.Z., O.R.-S. and L.O.; writing—original draft preparation, F.V. and L.O.; writing—review and editing, F.V., L.O. and O.R.-S.; supervision, L.O. All authors have read and agreed to the published version of the manuscript.

**Funding:** This research received no external funding.

**Institutional Review Board Statement:** Not applicable.

**Data Availability Statement:** Publicly available datasets were analyzed in this study. Raw data can be found at <https://www.ncbi.nlm.nih.gov/sra> accessed on 24 April 2020, with accession numbers indicated in the additional Table S2, whereas available CDS data can be found at <https://www.ncbi.nlm.nih.gov/genome/> accessed on 24 April 2020. The datasets generated and analyzed during the current study, when not available as supplementary information, and the associated scripts are available from the corresponding author on request.

**Acknowledgments:** We acknowledge the support of the Italian Ministry of Education, University and Research (MIUR) Dipartimenti di Eccellenza Program (2018–2022), Department of Biology and Biotechnology “L. Spallanzani”, University of Pavia.

**Conflicts of Interest:** The authors declare no conflict of interest.

## References

1. Bickel, D.; Pape, T.; Meier, R. *Diptera Diversity: Status, Challenges and Tools*; Brill: Leiden, The Netherlands, 2009; ISBN 978-90-04-18100-7.
2. Daane, K.M.; Johnson, M.W. Olive Fruit Fly: Managing an Ancient Pest in Modern Times. *Annu. Rev. Entomol.* **2010**, *55*, 151–169. [[CrossRef](#)] [[PubMed](#)]
3. Barr, N.B.; Ledezma, L.A.; Leblanc, L.; San Jose, M.; Rubinoff, D.; Geib, S.M.; Fujita, B.; Bartels, D.W.; Garza, D.; Kerr, P.; et al. Genetic Diversity of *Bactrocera dorsalis* (Diptera: Tephritidae) on the Hawaiian Islands: Implications for an Introduction Pathway Into California. *J. Econ. Entomol.* **2014**, *107*, 1946–1958. [[CrossRef](#)] [[PubMed](#)]
4. Vargas, R.I.; Nishida, T. Survey for *Dacus latifrons* (Diptera: Tephritidae). *J. Econ. Entomol.* **1985**, *78*, 1311–1314. [[CrossRef](#)]
5. Lux, S.A.; Copeland, R.S.; White, I.M.; Manrakhan, A.; Billah, M.K. A New Invasive Fruit Fly Species from the *Bactrocera dorsalis* (Hendel) Group Detected in East Africa. *Int. J. Trop. Insect Sci.* **2003**, *23*, 355–361. [[CrossRef](#)]
6. Drew, R.A.I.; Tsuruta, K.; White, I. A New Species of Pest Fruit Fly (Diptera: Tephritidae: Dacinae) from Sri Lanka and Africa. *Afr. Entomol.* **2004**, *13*, 149–154.
7. Vayssières, J.-F.; Goergen, G.; Lokossou, O.; Dossa, P.; Akponon, C. A New *Bactrocera* Species in Benin among Mango Fruit Fly (Diptera: Tephritidae) Species. *Fruits* **2005**, *60*, 371–377. [[CrossRef](#)]
8. Goergen, G.; Vayssières, J.-F.; Gnanvossou, D.; Tindo, M. *Bactrocera invadens* (Diptera: Tephritidae), a New Invasive Fruit Fly Pest for the Afrotropical Region: Host Plant Range and Distribution in West and Central Africa. *Env. Entomol.* **2011**, *40*, 844–854. [[CrossRef](#)] [[PubMed](#)]
9. EPPO Global Database. Available online: <https://gd.eppo.int> (accessed on 21 June 2022).
10. Crop Protection Compendium. Available online: <https://www.cabi.org/cpc> (accessed on 21 June 2022).

11. Mwatawala, M.; Makundi, R.; Maerere, A.P.; De Meyer, M. Occurrence of the Solanum Fruit Fly *Bactrocera latifrons* (Hendel) (Diptera: Tephritidae) in Tanzania. *J. Afrotrop. Zool.* **2010**, *6*, 83–89.
12. Mziray, H.A.; Makundi, R.H.; Mwatawala, M.; Maerere, A.; De Meyer, M. Host Use of *Bactrocera latifrons*, a New Invasive Tephritid Species in Tanzania. *J. Econ. Entomol.* **2010**, *103*, 70–76. [[CrossRef](#)]
13. Nugnes, F.; Russo, E.; Viggiani, G.; Bernardo, U. First Record of an Invasive Fruit Fly Belonging to *Bactrocera dorsalis* Complex (Diptera: Tephritidae) in Europe. *Insects* **2018**, *9*, 182. [[CrossRef](#)]
14. Gargiulo, S.; Nugnes, F.; Benedetta, F.; Bernardo, U. *Bactrocera latifrons* in Europe: The Importance of the Right Attractant for Detection. *Bull. Insectol.* **2021**, *74*, 311–320.
15. Doorenweerd, C.; Leblanc, L.; Norrbom, A.L.; San Jose, M.; Rubinoff, D. A Global Checklist of the 932 Fruit Fly Species in the Tribe Dacini (Diptera, Tephritidae). *ZooKeys* **2018**, *730*, 19–56. [[CrossRef](#)] [[PubMed](#)]
16. Vargas, R.I.; Piñero, J.C.; Leblanc, L. An Overview of Pest Species of *Bactrocera* Fruit Flies (Diptera: Tephritidae) and the Integration of Biopesticides with Other Biological Approaches for Their Management with a Focus on the Pacific Region. *Insects* **2015**, *6*, 297–318. [[CrossRef](#)] [[PubMed](#)]
17. White, I.M.; Elson-Harris, M.M. *Fruit Flies of Economic Significance: Their Identification and Bionomics*; CAB International: Wallingford, UK, 1992; ISBN 0-85198-790-7.
18. Ometto, L.; Cestaro, A.; Ramasamy, S.; Grassi, A.; Revadi, S.; Siozios, S.; Moretto, M.; Fontana, P.; Varotto, C.; Pisani, D.; et al. Linking Genomics and Ecology to Investigate the Complex Evolution of an Invasive *Drosophila* Pest. *Genome Biol. Evol.* **2013**, *5*, 745–757. [[CrossRef](#)] [[PubMed](#)]
19. Clarke, A.R.; Armstrong, K.F.; Carmichael, A.E.; Milne, J.R.; Raghu, S.; Roderick, G.K.; Yeates, D.K. Invasive Phytophagous Pests Arising through a Recent Tropical Evolutionary Radiation: The *Bactrocera dorsalis* Complex of Fruit Flies. *Annu. Rev. Entomol.* **2004**, *50*, 293–319. [[CrossRef](#)] [[PubMed](#)]
20. Drew, R.A.I. The Tropical Fruit Flies (Diptera: Tephritidae: Dacinae) of the Australasian Region and Oceanic Regions. *Mem. Qld. Mus.* **1989**, *26*, 1–521.
21. Drew, R.A.I.; Hancock, D.L. *Phylogeny of the Tribe Dacini (Dacinae) Based on Morphological, Distributional, and Biological Data*; CRC Press: Boca Raton, FL, USA, 1999; pp. 509–522. ISBN 978-0-429-12467-9.
22. Drew, R.A.I.; Romig, M.C. *Keys to the Tropical Fruit Flies of South-East Asia*; CABI: Wallingford, UK, 2016.
23. Krosch, M.N.; Schutze, M.K.; Armstrong, K.F.; Graham, G.C.; Yeates, D.K.; Clarke, A.R. A Molecular Phylogeny for the Tribe Dacini (Diptera: Tephritidae): Systematic and Biogeographic Implications. *Mol. Phylogenet. Evol.* **2012**, *64*, 513–523. [[CrossRef](#)]
24. San Jose, M.; Doorenweerd, C.; Leblanc, L.; Barr, N.; Geib, S.; Rubinoff, D. Incongruence between Molecules and Morphology: A Seven-Gene Phylogeny of Dacini Fruit Flies Paves the Way for Reclassification (Diptera: Tephritidae). *Mol. Phylogenet. Evol.* **2018**, *121*, 139–149. [[CrossRef](#)]
25. Virgilio, M.; Jordaens, K.; Verwimp, C.; White, I.M.; De Meyer, M. Higher Phylogeny of Frugivorous Flies (Diptera, Tephritidae, Dacini): Localised Partition Conflicts and a Novel Generic Classification. *Mol. Phylogenet. Evol.* **2015**, *85*, 171–179. [[CrossRef](#)]
26. Dupuis, J.R.; Bremer, F.T.; Kauwe, A.; San Jose, M.; Leblanc, L.; Rubinoff, D.; Geib, S.M. HiMAP: Robust Phylogenomics from Highly Multiplexed Amplicon Sequencing. *Mol. Ecol. Resour.* **2018**, *18*, 1000–1019. [[CrossRef](#)]
27. Muraji, M.; Nakahara, S. Phylogenetic Relationships among Fruit Flies, *Bactrocera* (Diptera, Tephritidae), Based on the Mitochondrial rDNA Sequences. *Insect Mol. Biol.* **2001**, *10*, 549–559. [[CrossRef](#)] [[PubMed](#)]
28. Nakahara, S.; Muraji, M. Phylogenetic Analyses of *Bactrocera* Fruit Flies (Diptera: Tephritidae) Based on Nucleotide Sequences of the Mitochondrial COI and COII Genes. *Res. Bull. Plant Prot. Jpn.* **2007**, *44*, 1–12.
29. Smith, P.T.; Kambhampati, S.; Armstrong, K.A. Phylogenetic Relationships among *Bactrocera* Species (Diptera: Tephritidae) Inferred from Mitochondrial DNA Sequences. *Mol. Phylogenet. Evol.* **2003**, *26*, 8–17. [[CrossRef](#)]
30. Yong, H.-S.; Song, S.-L.; Lim, P.-E.; Eamsobhana, P.; Suana, I.W. Complete Mitochondrial Genome of Three *Bactrocera* Fruit Flies of Subgenus *Bactrocera* (Diptera: Tephritidae) and Their Phylogenetic Implications. *PLoS ONE* **2016**, *11*, e0148201. [[CrossRef](#)]
31. Zhang, B.; Liu, Y.H.; Wu, W.X.; Wang, Z.L. Molecular Phylogeny of *Bactrocera* Species (Diptera: Tephritidae: Dacini) Inferred from Mitochondrial Sequences of 16S rDNA and COI Sequences. *Fla. Entomol.* **2010**, *93*, 369–377. [[CrossRef](#)]
32. Choo, A.; Nguyen, T.N.M.; Ward, C.M.; Chen, I.Y.; Sved, J.; Shearman, D.; Gilchrist, A.S.; Crisp, P.; Baxter, S.W. Identification of Y-Chromosome Scaffolds of the Queensland Fruit Fly Reveals a Duplicated Gyf Gene Parologue Common to Many *Bactrocera* Pest Species. *Insect Mol. Biol.* **2019**, *28*, 873–886. [[CrossRef](#)]
33. Papanicolaou, A.; Schetelig, M.F.; Arensburger, P.; Atkinson, P.W.; Benoit, J.B.; Bourtzis, K.; Castañera, P.; Cavanaugh, J.P.; Chao, H.; Childers, C.; et al. The Whole Genome Sequence of the Mediterranean Fruit Fly, *Ceratitis capitata* (Wiedemann), Reveals Insights into the Biology and Adaptive Evolution of a Highly Invasive Pest Species. *Genome Biol.* **2016**, *17*, 192. [[CrossRef](#)]
34. Sim, S.B.; Geib, S.M. A Chromosome-Scale Assembly of the *Bactrocera cucurbitae* Genome Provides Insight to the Genetic Basis of White Pupae. *G3 Genes Genomes Genet.* **2017**, *7*, 1927–1940. [[CrossRef](#)]
35. Geib, S.M.; Calla, B.; Hall, B.; Hou, S.; Manoukis, N.C. Characterizing the Developmental Transcriptome of the Oriental Fruit Fly, *Bactrocera dorsalis* (Diptera: Tephritidae) through Comparative Genomic Analysis with *Drosophila melanogaster* Utilizing ModENCODE Datasets. *BMC Genom.* **2014**, *15*, 924. [[CrossRef](#)]
36. Wang, J.; Xiong, K.-C.; Liu, Y.-H. De Novo Transcriptome Analysis of Chinese Citrus Fly, *Bactrocera minax* (Diptera: Tephritidae), by High-Throughput Illumina Sequencing. *PLoS ONE* **2016**, *11*, e0157656. [[CrossRef](#)]

37. Bayega, A.; Djambazian, H.; Tsoumani, K.T.; Gregoriou, M.E.; Sagri, E.; Drosopoulou, E.; Mavragani-Tsipidou, P.; Giorda, K.; Tsiamis, G.; Bourtzis, K.; et al. De Novo Assembly of the Olive Fruit Fly (*Bactrocera oleae*) Genome with Linked-Reads and Long-Read Technologies Minimizes Gaps and Provides Exceptional y Chromosome Assembly. *BMC Genom.* **2020**, *21*, 259. [[CrossRef](#)] [[PubMed](#)]
38. Grabherr, M.G.; Haas, B.J.; Yassour, M.; Levin, J.Z.; Thompson, D.A.; Amit, I.; Adiconis, X.; Fan, L.; Raychowdhury, R.; Zeng, Q.; et al. Full-Length Transcriptome Assembly from RNA-Seq Data without a Reference Genome. *Nat. Biotechnol.* **2011**, *29*, 644–652. [[CrossRef](#)] [[PubMed](#)]
39. Camacho, C.; Coulouris, G.; Avagyan, V.; Ma, N.; Papadopoulos, J.; Bealer, K.; Madden, T.L. BLAST+: Architecture and Applications. *BMC Bioinform.* **2009**, *10*, 421. [[CrossRef](#)]
40. Katoh, K.; Standley, D.M. MAFFT Multiple Sequence Alignment Software Version 7: Improvements in Performance and Usability. *Mol. Biol. Evol.* **2013**, *30*, 772–780. [[CrossRef](#)]
41. Löytynoja, A.; Goldman, N. A Model of Evolution and Structure for Multiple Sequence Alignment. *Philos. Trans. R. Soc. B Biol. Sci.* **2008**, *363*, 3913–3919. [[CrossRef](#)]
42. Abascal, F.; Zardoya, R.; Telford, M.J. TranslatorX: Multiple Alignment of Nucleotide Sequences Guided by Amino Acid Translations. *Nucleic Acids Res.* **2010**, *38*, W7–W13. [[CrossRef](#)]
43. Ramasamy, S.; Ometto, L.; Crava, C.M.; Revadi, S.; Kaur, R.; Horner, D.S.; Pisani, D.; Dekker, T.; Anfora, G.; Rota-Stabelli, O. The Evolution of Olfactory Gene Families in *Drosophila* and the Genomic Basis of Chemical-Ecological Adaptation in *Drosophila suzukii*. *Genome Biol. Evol.* **2016**, *8*, 2297–2311. [[CrossRef](#)]
44. Kumar, S.; Stecher, G.; Tamura, K. MEGA7: Molecular Evolutionary Genetics Analysis Version 7.0 for Bigger Datasets. *Mol. Biol. Evol.* **2016**, *33*, 1870–1874. [[CrossRef](#)]
45. Stamatakis, A. RAxML Version 8: A Tool for Phylogenetic Analysis and Post-Analysis of Large Phylogenies. *Bioinformatics* **2014**, *30*, 1312–1313. [[CrossRef](#)]
46. Zhang, C.; Rabiee, M.; Sayyari, E.; Mirarab, S. ASTRAL-III: Polynomial Time Species Tree Reconstruction from Partially Resolved Gene Trees. *BMC Bioinform.* **2018**, *19*, 153. [[CrossRef](#)]
47. Bouckaert, R.; Vaughan, T.G.; Barido-Sottani, J.; Duchêne, S.; Fourment, M.; Gavryushkina, A.; Heled, J.; Jones, G.; Kühnert, D.; De Maio, N.; et al. BEAST 2.5: An Advanced Software Platform for Bayesian Evolutionary Analysis. *PLoS Comput. Biol.* **2019**, *15*, e1006650. [[CrossRef](#)] [[PubMed](#)]
48. Lartillot, N.; Philippe, H. A Bayesian Mixture Model for Across-Site Heterogeneities in the Amino-Acid Replacement Process. *Mol. Biol. Evol.* **2004**, *21*, 1095–1109. [[CrossRef](#)] [[PubMed](#)]
49. Ogilvie, H.A.; Bouckaert, R.R.; Drummond, A.J. StarBEAST2 Brings Faster Species Tree Inference and Accurate Estimates of Substitution Rates. *Mol. Biol. Evol.* **2017**, *34*, 2101–2114. [[CrossRef](#)]
50. Barido-Sottani, J.; Bošková, V.; Du Plessis, L.; Kühnert, D.; Magnus, C.; Mitov, V.; Müller, N.F.; Pečerska, J.; Rasmussen, D.A.; Zhang, C.; et al. Taming the BEAST—A Community Teaching Material Resource for BEAST 2. *Syst. Biol.* **2018**, *67*, 170–174. [[CrossRef](#)] [[PubMed](#)]
51. Bouckaert, R.R.; Heled, J. DensiTree 2: Seeing Trees Through the Forest. *bioRxiv* **2014**, 012401. [[CrossRef](#)]
52. Norrbom, A. New Genera of Tephritidae (Diptera) from Brazil and Dominican Amber, with Phylogenetic Analysis of the Tribe Ortalotrypetini. *Insecta Mundi* **1994**, *8*, 1–15.
53. Wiegmann, B.M.; Trautwein, M.D.; Winkler, I.S.; Barr, N.B.; Kim, J.-W.; Lambkin, C.; Bertone, M.A.; Cassel, B.K.; Bayless, K.M.; Heimberg, A.M.; et al. Episodic Radiations in the Fly Tree of Life. *Proc. Natl. Acad. Sci. USA* **2011**, *108*, 5690–5695. [[CrossRef](#)]
54. Junqueira, A.C.M.; Azeredo-Espin, A.M.L.; Paulo, D.F.; Marinho, M.A.T.; Tomsho, L.P.; Drautz-Moses, D.I.; Purbojati, R.W.; Ratan, A.; Schuster, S.C. Large-Scale Mitogenomics Enables Insights into Schizophora (Diptera) Radiation and Population Diversity. *Sci. Rep.* **2016**, *6*, 1–13. [[CrossRef](#)]
55. Keightley, P.D.; Trivedi, U.; Thomson, M.; Oliver, F.; Kumar, S.; Blaxter, M.L. Analysis of the Genome Sequences of Three *Drosophila melanogaster* Spontaneous Mutation Accumulation Lines. *Genome Res.* **2009**, *19*, 1195–1201. [[CrossRef](#)]
56. Obbard, D.J.; Maclennan, J.; Kim, K.-W.; Rambaut, A.; O’Grady, P.M.; Jiggins, F.M. Estimating Divergence Dates and Substitution Rates in the *Drosophila* Phylogeny. *Mol. Biol. Evol.* **2012**, *29*, 3459–3473. [[CrossRef](#)]
57. Keightley, P.D.; Pinharanda, A.; Ness, R.W.; Simpson, F.; Dasmahapatra, K.K.; Mallet, J.; Davey, J.W.; Jiggins, C.D. Estimation of the Spontaneous Mutation Rate in *Heliconius melpomene*. *Mol. Biol. Evol.* **2015**, *32*, 239–243. [[CrossRef](#)] [[PubMed](#)]
58. Keightley, P.D.; Ness, R.W.; Halligan, D.L.; Haddrill, P.R. Estimation of the Spontaneous Mutation Rate per Nucleotide Site in a *Drosophila melanogaster* Full-Sib Family. *Genetics* **2014**, *196*, 313–320. [[CrossRef](#)] [[PubMed](#)]
59. Vargas, R.I.; Walsh, W.A.; Kanehisa, D.; Jang, E.B.; Armstrong, J.W. Demography of Four Hawaiian Fruit Flies (Diptera: Tephritidae) Reared at Five Constant Temperatures. *Ann. Entomol. Soc. Am.* **1997**, *90*, 162–168. [[CrossRef](#)]
60. Stephens, A.E.A.; Kriticos, D.J.; Leriche, A. The Current and Future Potential Geographical Distribution of the Oriental Fruit Fly, *Bactrocera dorsalis* (Diptera: Tephritidae). *Bull. Entomol. Res.* **2007**, *97*, 369–378. [[CrossRef](#)]
61. Theron, C.D.; Manrakhan, A.; Weldon, C.W. Host Use of the Oriental Fruit Fly, *Bactrocera dorsalis* (Hendel) (Diptera: Tephritidae), in South Africa. *J. Appl. Entomol.* **2017**, *141*, 810–816. [[CrossRef](#)]
62. Li, X.; Yang, H.; Wang, T.; Wang, J.; Wei, H. Life History and Adult Dynamics of *Bactrocera dorsalis* in the Citrus Orchard of Nanchang, a Subtropical Area from China: Implications for a Control Timeline. *ScienceAsia* **2019**, *45*, 212–220. [[CrossRef](#)]

63. Russel, P.M.; Brewer, B.J.; Klaere, S.; Bouckaert, R.R. Model Selection and Parameter Inference in Phylogenetics Using Nested Sampling. *Syst. Biol.* **2019**, *68*, 219–233. [[CrossRef](#)]
64. Kass, R.E.; Raftery, A.E. Bayes Factors. *J. Am. Stat. Assoc.* **1995**, *90*, 774–795. [[CrossRef](#)]
65. Schrempf, D.; Minh, B.Q.; De Maio, N.; von Haeseler, A.; Kosiol, C. Reversible Polymorphism-Aware Phylogenetic Models and Their Application to Tree Inference. *J. Theor. Biol.* **2016**, *407*, 362–370. [[CrossRef](#)]
66. Drew, R.A.I.; Lambert, D.M. On the Specific Status of *Dacus* (*Bactrocera*) *aquilonis* and *D.* (*Bactrocera*) *tryoni* (Diptera: Tephritidae). *Ann. Entomol. Soc. Am.* **1986**, *79*, 870–878. [[CrossRef](#)]
67. Cruickshank, L.; Jessup, A.J.; Cruickshank, D.J. Interspecific Crosses of *Bactrocera tryoni* (Froggatt) and *Bactrocera jarvisi* (Tryon) (Diptera: Tephritidae) in the Laboratory. *Aust. J. Entomol.* **2001**, *40*, 278–280. [[CrossRef](#)]
68. Pike, N.; Wang, W.Y.S.; Meats, A. The Likely Fate of Hybrids of *Bactrocera tryoni* and *Bactrocera neohumeralis*. *Heredity* **2003**, *90*, 365–370. [[CrossRef](#)] [[PubMed](#)]
69. Wee, S.-L.; Tan, K.-H. Evidence of Natural Hybridization between Two Sympatric Sibling Species of *Bactrocera dorsalis* Complex Based on Pheromone Analysis. *J. Chem. Ecol.* **2005**, *31*, 845–858. [[CrossRef](#)] [[PubMed](#)]
70. Ebina, T.; Ohto, K. Morphological Characters and PCR-RFLP Markers in the Interspecific Hybrids between *Bactrocera carambolae* and *B. papayae* of the *B. dorsalis* Species Complex (Diptera: Tephritidae). *Res. Bull. Plant Prot. Serv. Jpn.* **2006**, *42*, 23–34.
71. Shearman, D.C.A.; Frommer, M.; Morrow, J.L.; Raphael, K.A.; Gilchrist, A.S. Interspecific Hybridization as a Source of Novel Genetic Markers for the Sterile Insect Technique in *Bactrocera tryoni* (Diptera: Tephritidae). *J. Econ. Entomol.* **2010**, *103*, 1071–1079. [[CrossRef](#)]
72. Schutze, M.K.; Jessup, A.; Ul-Haq, I.; Vreysen, M.J.B.; Wornoayporn, V.; Vera, M.T.; Clarke, A.R. Mating Compatibility Among Four Pest Members of the *Bactrocera dorsalis* Fruit Fly Species Complex (Diptera: Tephritidae). *J. Econ. Entomol.* **2013**, *106*, 695–707. [[CrossRef](#)]
73. Augustinos, A.A.; Drosopoulou, E.; Gariou-Papalexioy, A.; Bourtzis, K.; Mavragani-Tsipidou, P.; Zacharopoulou, A. The *Bactrocera dorsalis* Species Complex: Comparative Cytogenetic Analysis in Support of Sterile Insect Technique Applications. *BMC Genet.* **2014**, *15*, S16. [[CrossRef](#)]
74. Bo, W.; Ahmad, S.; Dammalage, T.; Tomas, U.S.; Wornoayporn, V.; Ul Haq, I.; Cáceres, C.; Vreysen, M.J.B.; Schutze, M.K. Mating Compatibility between *Bactrocera invadens* and *Bactrocera dorsalis* (Diptera: Tephritidae). *J. Econ. Entomol.* **2014**, *107*, 623–629. [[CrossRef](#)]
75. Gilchrist, A.S.; Shearman, D.C.; Frommer, M.; Raphael, K.A.; Deshpande, N.P.; Wilkins, M.R.; Sherwin, W.B.; Sved, J.A. The Draft Genome of the Pest Tephritid Fruit Fly *Bactrocera tryoni*: Resources for the Genomic Analysis of Hybridising Species. *BMC Genom.* **2014**, *15*, 1153. [[CrossRef](#)]
76. Yeap, H.L.; Lee, S.F.; Robinson, F.; Mourant, R.G.; Sved, J.A.; Frommer, M.; Papanicolaou, A.; Edwards, O.R.; Oakeshott, J.G. Separating Two Tightly Linked Species-Defining Phenotypes in *Bactrocera* with Hybrid Recombinant Analysis. *BMC Genet.* **2020**, *21*, 132. [[CrossRef](#)]
77. Pollard, D.A.; Iyer, V.N.; Moses, A.M.; Eisen, M.B. Widespread Discordance of Gene Trees with Species Tree in *Drosophila*: Evidence for Incomplete Lineage Sorting. *PLoS Genet.* **2006**, *2*, e173. [[CrossRef](#)] [[PubMed](#)]
78. Yaakop, S.; Ibrahim, N.J.; Shariff, S.; Zain, B.M.M. Molecular Clock Analysis on Five *Bactrocera* Species Flies (Diptera: Tephritidae) Based on Combination of COI and NADH Sequences. *Orient. Insects* **2015**, *49*, 150–164. [[CrossRef](#)]
79. Nardi, F.; Carapelli, A.; Boore, J.L.; Roderick, G.K.; Dallai, R.; Frati, F. Domestication of Olive Fly through a Multi-Regional Host Shift to Cultivated Olives: Comparative Dating Using Complete Mitochondrial Genomes. *Mol. Phylogenet. Evol.* **2010**, *57*, 678–686. [[CrossRef](#)] [[PubMed](#)]
80. Zhong, G.; Geng, J.; Wong, H.K.; Ma, Z.; Wu, N. A Semi-Quantitative Method for the Reconstruction of Eustatic Sea Level History from Seismic Profiles and Its Application to the Southern South China Sea. *Earth Planet. Sci. Lett.* **2004**, *223*, 443–459. [[CrossRef](#)]
81. DeSalle, R.; Giddings, L.V. Discordance of Nuclear and Mitochondrial DNA Phylogenies in Hawaiian *Drosophila*. *Proc. Natl. Acad. Sci. USA* **1986**, *83*, 6902–6906. [[CrossRef](#)]
82. Beltrán, M.; Jiggins, C.D.; Bull, V.; Linares, M.; Mallet, J.; McMillan, W.O.; Bermingham, E. Phylogenetic Discordance at the Species Boundary: Comparative Gene Genealogies Among Rapidly Radiating *Heliconius* Butterflies. *Mol. Biol. Evol.* **2002**, *19*, 2176–2190. [[CrossRef](#)]
83. Putnam, A.S.; Scriber, J.M.; Andolfatto, P. Discordant Divergence Times among Z-Chromosome Regions between Two Ecologically Distinct Swallowtail Butterfly Species. *Evolution* **2007**, *61*, 912–927. [[CrossRef](#)]
84. Toews, D.P.L.; Brelsford, A. The Biogeography of Mitochondrial and Nuclear Discordance in Animals. *Mol. Ecol.* **2012**, *21*, 3907–3930. [[CrossRef](#)]
85. Drummond, A.J.; Ho, S.Y.W.; Phillips, M.J.; Rambaut, A. Relaxed Phylogenetics and Dating with Confidence. *PLoS Biol.* **2006**, *4*, e88. [[CrossRef](#)]
86. Ho, S.Y.W.; Lanfear, R.; Bromham, L.; Phillips, M.J.; Soubrier, J.; Rodrigo, A.G.; Cooper, A. Time-Dependent Rates of Molecular Evolution. *Mol. Ecol.* **2011**, *20*, 3087–3101. [[CrossRef](#)]
87. Ho, S.Y.W.; Lo, N. The Insect Molecular Clock. *Aust. J. Entomol.* **2013**, *52*, 101–105. [[CrossRef](#)]
88. Misof, B.; Liu, S.; Meusemann, K.; Peters, R.S.; Donath, A.; Mayer, C.; Frandsen, P.B.; Ware, J.; Flouri, T.; Beutel, R.G.; et al. Phylogenomics Resolves the Timing and Pattern of Insect Evolution. *Science* **2014**, *346*, 763–767. [[CrossRef](#)] [[PubMed](#)]